Electrochimica Acta 563 (2026) 148692

Contents lists available at ScienceDirect

Electrochimica Acta

journal homepage: www.journals.elsevier.com/electrochimica-acta

Wearable paper-based potentiometric sensor for real-time detection of chloride ions in sweat

Luca Fiore [a,b], Giorgia Leotta [a], Matteo di Carmine [b], Arianna Antinucci [b], Florigio Lista [c], Fabiana Arduini [a,b,*]

[a] Department of Chemical Science and Technologies, University of Rome "Tor Vergata", Via della Ricerca Scientifica 1, Rome 00133, Italy
[b] SENSE4MED, Via Bitonto 139, 00133 Rome, Italy
[c] Defence Institute for Biomedical Sciences, Via S. Stefano Rotondo 4, 00184 Rome, Italy

ARTICLE INFO

Keywords:
Solid-contact ion-selective electrode
Capillary-driven microfluidics
All-solid-state reference electrode
Sweat electrolyte monitoring
Hysteresis-free sensing
Carbon black

ABSTRACT

Herein, we report an office-paper-based potentiometric sensor integrated with a microfluidic paper network in an *apple-like* configuration, designed for continuous monitoring of chloride ions in sweat within a wearable platform. The paper-based device combines a chloride-selective membrane with a solid-contact, office paper-screen-printed transducer, and a capillary-driven paper-based microfluidic architecture, ensuring controlled sample delivery, minimising evaporation-induced drift, and eliminating memory effects, as confirmed by hysteresis studies. This work highlights the effectiveness of paper as a smart material for both sensing and sweat management in wearable electrochemical devices, achieving a sensitivity of 56 mV/log a Cl^-, a linear range of 1–200 mmol L^{-1}, and a detection limit of 74 μmol L^{-1} in artificial sweat. Compared with the reference titration method, bias values ranged from −14% to +4%. These results pave the way for low-cost, disposable, environmentally friendly, and memory-free evaluation of electrolyte balance during physical activity, as well as for non-invasive diagnostics and monitoring highly effective modulator therapy in cystic fibrosis.

1. Introduction

In 2017, the World Economic Forum highlighted liquid biopsy as one of the Top 10 Emerging Technologies because it enables the detection of circulating biomolecules such as cf-DNA, miRNA, and proteins, offering high specificity and systemic insight for disease diagnosis and therapy monitoring [1]. However, it requires venipuncture, specialized laboratory infrastructure, and trained personnel, which limits its use for continuous monitoring.

Beyond liquid biopsy, sweat analysis has gained attention over the last decade because it offers a non-invasive approach to monitoring physiological and biochemical status [2]. Sweat contains electrolytes and metabolites that reflect hydration status, metabolic activity, and changes related to disease. The effectiveness of sweat as a matrix and the recent advancements in wearable technologies have fostered the development of a new concept in electrochemical devices, transitioning from point-of-care devices, such as glucose strips, to wearable devices for continuous and non-invasive monitoring of sweat biomarkers.

Among the various analytes present in sweat, chloride ions are key biomarkers for assessing both physiological and pathological conditions. Chloride ions are one of the principal electrolytes in human sweat; the physiological chloride concentration in sweat is in the range 0-150 mmol L^{-1} and is typically present at concentrations below 30 mmol L^{-1} in healthy individuals under normal conditions [3–6]. Variability in sweat chloride ion content reflects differences in sweat rate and exercise intensity; for instance, the Searson group [7] reported a real-time sweat chloride ion content for 12 healthy subjects by increasing the exercise load from 100 W to 200 W, observing that sweat chloride ion concentration increased from 12.0 ± 5.9 to 31.4 ± 16 mmol L^{-1}. Conversely, decreasing the load from 200 W to 100 W, the sweat chloride ion content decreased from 27.7 ± 10.5 to 14.8 ± 8.1 mmol L^{-1}, noting a dynamic sweat chloride response related to step changes in exercise load. In this way, changes in sweat chloride ion content correlate with shifts in electrolyte losses during prolonged activity and thermal stress and can therefore serve as a biomarker of overall electrolyte balance during exercise [8].

In the clinical field, the gold standard method that uses sweat as a matrix is the sweat test used for the diagnosis of cystic fibrosis, a genetic

* Corresponding author.
E-mail address: fabiana.arduini@uniroma2.it (F. Arduini).

https://doi.org/10.1016/j.electacta.2026.148692
Received 15 January 2026; Received in revised form 6 March 2026; Accepted 15 March 2026
Available online 17 March 2026

disorder caused by impaired CFTR-mediated chloride transport [4,5,9]. According to established clinical guidelines, sweat chloride concentrations ≥60 mmol L^{-1} are diagnostic for cystic fibrosis [10]. Moreover, the advent of CFTR modulators has highlighted that the sweat test can also be used as an outcome measure to monitor the efficacy of these new drugs in restoring the basic defect of CFTR [11,12]. The test is carried out by stimulating sweat production using pilocarpine iontophoresis, followed by the collection of sweat on a pre-weighed gauze/paper or using a specialised sweat collector (Macroduct® coil system) placed over the stimulated area. Subsequently, the collected sweat is analysed by coulometric titration or other validated quantitative methods [10].

In this overall scenario, accurate, real-time monitoring of sweat chloride ions can enable early detection of abnormalities and support continuous health assessment. The constraints of conventional clinical methods, including centralised instrumentation and controlled laboratory conditions, hinder decentralised testing and continuous monitoring, motivating the development of miniaturised electrochemical sensors capable of providing real-time and low-volume measurements. Among miniaturised electrochemical sensors, potentiometric ion-selective electrodes (ISEs) remain particularly attractive due to their Nernstian response, low power consumption, and direct transduction of ionic activity into an electrical signal.

Early efforts toward chloride ion sensing in sweat focused on flexible solid-contact ISEs have been reported in the literature. For instance, Choi et al. [13] developed a 125 μm thick PET-based potentiometric device with an Ag film patterned on PET with an integrated salt bridge that minimises equilibration and enables stable measurements, with variation of less than 2 mmol L^{-1} at low chloride ions concentration (10 mmol L^{-1}) and 5 mmol L^{-1} at high concentration (150 mmol L^{-1}). While analytically robust, this approach lacked integrated fluid-handling elements, making measurements subject to sample variability and evaporation effects.

Wang et al. [14] developed an all-solid-state chloride-selective electrode based on oxygen vacancies-reinforced vanadium oxide with a nitrogen-doped carbon shield as the solid contact, characterised by a low detection limit of $10^{-5.45}$ mol L^{-1} without an interfacial water layer and highly stable potential with 7.24 μV/h over 24 h. The PDMS-based microfluidic channels were designed and demolded, followed by treatment with oxygen plasma and a 1% 3-aminopropyltriethoxysilane solution via spray coating for hydrophilic modification.

To overcome the limitations of conventional PDMS-based microfluidics, paper has emerged as an attractive alternative due to its versatile features. Its fibrous structure not only supports sustainable and low-cost fabrication but also enables capillary-driven fluid transport, allowing sweat samples to flow naturally without the need for external pumps and thereby avoiding the issue of bubbles. Additionally, paper can store reagents within its matrix, facilitating reagent-free measurements, and it eliminates the need for complex sample pretreatment such as filtration [15]. These properties make paper-based microfluidic platforms particularly useful for wearable and real-time sweat analysis, providing a simple, robust, and fully integrated system for continuous monitoring of sweat biomarkers such as chloride ions.

In this regard, Shitanda et al. [16] developed a wearable PET-based screen-printed ion sensor fabricated using a heat-transfer-printed sensor, combined with superabsorbent fibres attached to the sensor cloth to continuously remove old sweat from the sensing part of the sensor. The chloride ion sensor showed a Nernst response of −59.5 mV/log c Cl^- in the 0.1−100 mmol L^{-1} concentration range, and the on-body test highlighted an increase in chloride ions in sweat with exercise time.

Bruno et al. [17] recently reported a paper-based microfluidic electrochemical sensor for chloride ion and uric acid detection in sweat with a handheld device, using chronoamperometry as a technique. The artificial sweat was managed using a layer of paper between two vinyl layers embedded in a PMMA, obtaining a linear range and sensitivity in artificial sweat equal to 1–100 mmol L^{-1} and 1.44 μA mmol L^{-1}, respectively. This device demonstrated the utility of the paper in managing sweat without an external pump but using a point-of-care device with already collected sweat samples.

Henry's group [18,19] reported paper-based colorimetric platforms for chloride ion determination, exploiting chromogenic reactions on patterned paper substrates. In these studies, chloride ion quantification was achieved through visual or smartphone-assisted color analysis, with reported linear range up to 50 mmol L^{-1} and detection limit of 160 μmol L^{-1}. While this approach demonstrated the feasibility of low-cost paper-based chloride analysis, it relied on endpoint colorimetric detection and was not designed for continuous, real-time wearable monitoring.

Herein, we present the first fully paper-based potentiometric chloride sensor integrated with a microfluidic paper network, specifically designed to enable continuous chloride ion detection using a wearable device. This analytical tool combines a chloride-selective membrane with a solid-contact, office paper-based screen-printed transducer, a capillary-driven paper-based microfluidic architecture, and a Bluetooth-enabled wearable potentiostat, ensuring controlled sample delivery, minimising evaporation-induced drift, and avoiding the memory effect, as demonstrated through hysteresis studies. The electrochemical performance of the sensor was systematically evaluated in terms of sensitivity, linear range, selectivity, response time, and potential stability. Its applicability is demonstrated through on-body measurements compared with the titration reference method. This approach advances the state of the art by enabling real-time, memory-free, and low-cost sweat chloride analysis.

2. Experimental section

2.1. Reagents and equipment

Carbon Black (CB) N220 was obtained from Cabot Corporation (Ravenna, Italy). Potassium chloride, sodium chloride, sodium acetate, urea, potassium nitrate, sodium-L-lactate, glucose, ammonium sulphate, acetic acid ≥ 99.7%, chloride ionophore I- cocktail A, dimethylformamide, polyvinyl butyral, polyvinyl chloride, and tetrahydrofuran were purchased from Sigma Aldrich (USA). A wax printer, ColoQube 8580 Xerox (USA), was used for printing wax patterns, while a laser cutter, VEVOR 40, was used for producing paper-based microfluidics. Office paper (Fabriano Copy 2, 80 g/m^2) was used as a paper substrate to print the electrodes. Graphite-based ink (Elettrodag 421 SS) and silver/silver chloride-based ink (Elettrodag 4038 SS) were purchased from Acheson Henkel (UK). Electrochemical impedance spectroscopy (EIS) and potentiometry were performed using an Emstat blue potentiostat (PalmSens, Netherlands) connected to a laptop and controlled by PSTrace 5.9 software. The Sensit wearable development kit (PalmSens, Netherlands) was used for wearable measurements.

2.2. Fabrication of office paper-based sensor

The paper-based electrochemical sensor for chloride ion detection was fabricated through a simple, scalable multi-step process involving wax patterning, screen-printing of electrodes, and drop-casting modification on office paper, following previously reported fabrication procedures [20–23]. First, hydrophobic patterns were designed using a vector drawing software (Adobe Illustrator) and printed onto office paper (Fabriano Copy 2, 80 g m^{-2}) using a solid-ink office wax printer (ColorQube 8580, Xerox, USA). The printed sheets were then thermally treated in an oven at 100 °C for 1 minute to allow the wax to melt and penetrate through the thickness of the paper, thereby creating well-defined hydrophobic barriers. This step enabled the formation of confined sensing zones, ensuring mechanical robustness and resistance to aqueous environments during measurements. After wax patterning, the electrode system was fabricated by screen-printing using custom-designed masks and commercial conductive inks. The

conductive tracks and the pseudo-reference electrode were first printed using a silver/silver chloride ink (Elettrodag 4038 SS), with the pseudo-reference electrode aligned within the wax-defined hydrophobic area, thereby maintaining a controlled and reproducible sensing region. The printed layers were cured at 70 °C for 20 min to promote solvent evaporation and resin polymerisation, ensuring good adhesion to the paper substrate and stable electrochemical properties. Subsequently, the working electrode was printed using a graphite-based ink (Elettrodag 421 SS) following the same screen-printing procedure. While the active electrode areas were located within the wax-patterned region, the conductive tracks were intentionally extended beyond the hydrophobic barriers to improve electrical conductivity and facilitate external connections. A second curing step was performed at 70 °C for 40 min to complete ink consolidation.

2.3. Preparation of carbon black dispersion

CB powder was dispersed in a mixture of dimethylformamide/water in a ratio of 1:1 (v/v) at a final concentration of 1 mg mL^{-1}. In detail, 10 mg of CB were added to 5 mL of dimethylformamide, and then 5 mL of water was added. The dispersion was sonicated for 60 min at 59 kHz [24].

2.4. Preparation of chloride ion-selective membrane and reference membrane

The chloride-selective membrane was prepared following a procedure adapted from existing ionophore-based formulations. In detail, the membrane cocktail consisted of 70% (w/w) chloride ionophore I–cocktail A and 30% (w/w) high molecular weight poly(vinyl chloride) (PVC). To this mixture, 1 mL of tetrahydrofuran (THF) was added per 100 mg of solid components. The resulting solution was magnetically stirred for 1 h to ensure complete homogenisation [25]. To prevent solvent-induced degradation of the vial cap caused by THF, a Teflon film was placed between the membrane solution and the cap, thereby preserving the container's integrity throughout the preparation process. The reference membrane was prepared following the procedure described by Gao et al. [26]. In detail, 237.3 mg of poly(vinyl butyral) (PVB) were dissolved in 3 mL of methanol, and 150 mg of NaCl were subsequently dispersed into the polymer solution under magnetic stirring. Upon solvent evaporation, NaCl became embedded within the PVB matrix, forming the solid-state reference membrane.

2.5. Paper-based screen-printed electrode modification

Working and pseudo-reference electrodes were functionalized by drop-casting appropriate modifier solutions. The working electrode was modified with a CB dispersion to enhance ion-to-electron transduction. The CB layer acts as a high-surface-area capacitive solid-contact, forming an electrical double layer at the interface between the electronic conductor and the ion-selective membrane. This interfacial capacitance enhances ion-to-electron transduction by providing efficient charge buffering, thereby improving potential stability and reducing signal drift. Moreover, the defective and highly porous carbon nanomaterial provides abundant surface-active sites that promote efficient charge transfer and help suppress the formation of an interfacial water layer [24,27]. The effectiveness of the CB modification is supported by EIS measurements (Fig. S1), which show a significant increase in low-frequency capacitance compared to the unmodified electrode. In detail, a total volume of 6 μL of CB dispersion was deposited in three successive aliquots of 2 μL, allowing each layer to dry for 30 min at room temperature. The pseudo-reference electrode was modified by drop-casting 2 μL of the reference membrane solution in two steps, followed by drying at room temperature for 10 min. After drying, the surface of the pseudo-reference electrode was conditioned by 10 μL of KCl 3 mol L^{-1} [24,28] solution for 2 hours in a humid chamber. The humid chamber was created by placing a moistened tissue in a Petri dish. This step was necessary to ensure the correct functioning of the pseudo-reference electrode, so that it remained constant during the analysis, even in contact with different ion strengths present in the sweat matrix. Subsequently, 5 μL of the chloride-selective membrane solution was drop-cast onto the CB-modified working electrode in two separate layers of 2.5 μL each, with a 20-minute drying interval between applications. The membrane on the working electrode was then conditioned to ensure a stable Nernstian response. For this purpose, a 1 mol L^{-1} NaCl solution was selected and 20 μL was carefully dropped onto the electrode surface. The conditioning process lasted 30 minutes and was conducted in a humid chamber, as was the case for the pseudo-reference electrode. Both membranes were subsequently rinsed with 20 μL of distilled water to remove excess salts.

2.6. Fabrication of paper-based microfluidics

The paper-based microfluidic device was fabricated using a CO_2 laser cutter with a VEVOR 40 W laser. Commercial tissue paper (Cordenons, Italy) was selected as the substrate due to its high capillary absorption capacity, which enables efficient, passive fluid transport without the need for an external pump. The microfluidic layout was designed using a vector graphics software (Adobe Illustrator) and subsequently transferred onto the paper substrate by laser cutting. The geometry was optimised to promote continuous capillary-driven flow and consisted of a circular sampling area with a diameter of 6 mm connected to an enlarged, apple-shaped waste reservoir through a narrow channel. The overall length of the microfluidic path was 63 mm, while the waste zone had a diameter of 47 mm. This configuration enables the continuous absorption of the fluid from the sensing area toward the waste zone, allowing for unidirectional flow and efficient removal of the analysed sample during measurements. The microfluidic paper layer was simply placed onto the electrode surface, aligning the sampling zone with the working and reference electrodes, thus forming a fully paper-based, pump-free microfluidic interface suitable for wearable and continuous sensing applications.

2.7. Potentiometric measurements of chloride ions in standard solutions

Potentiometric measurements were carried out using a portable PalmSens potentiostat in Open Circuit Potentiometry (OCP) mode, applying the following parameters: t interval = 0.1 s and t run = 10 s. The measurements were performed by drop-casting 50 μL of each standard solution directly onto the same sensing electrode surface. All measurements were conducted in triplicate.

2.8. Potentiometric measurements of chloride ions in sweat

To evaluate the electrochemical performance of the sensor in sweat, measurements were performed using both artificial and real sweat samples. Prior to real-sample analysis, the sensor was calibrated using artificial sweat solutions with increasing chloride concentrations, ranging from 1 to 200 mmol L^{-1}. For these measurements, the paper-based microfluidic pad was placed on top of the electrode surface, and the calibration solutions were applied to fully wet the microfluidic pattern. Artificial sweat was prepared considering the range values of the biomarkers reported in [29]. In detail, the solution contained ammonium sulphate (0.25 mmol L^{-1}), potassium nitrate (6 mmol L^{-1}), glucose (0.3 mmol L^{-1}), urea (3 mmol L^{-1}), and sodium lactate (25 mmol L^{-1}). All components were dissolved in acetate buffer at pH 5.5 to reproduce the typical pH of human sweat. Following calibration, the sensor was used for measurements of real sweat samples collected from three volunteer participants. For each measurement, only 10 μL of sweat was enough to completely wet the paper-based microfluidic pad, allowing potentiometric measurements under low sample volume conditions. The chloride ion concentration in sweat samples was

determined using the calibration curve obtained in artificial sweat.

2.9. Potentiometric measurements of chloride ions in sweat using a wearable system

For wearable measurements, the developed paper-based chloride-selective sensor was integrated into a compact wireless potentiometric system (Sensit/Wearable development kit, PalmSens, The Netherlands). The device enables real-time signal acquisition and wireless data transmission to a smartphone through a dedicated application, allowing on-body measurements without the need for external instrumentation. Prior to use, the paper-based sensor was electrically connected to the wearable module. The paper-based microfluidic pad was then positioned on top of the sensing area, aligned with the working and pseudo-reference electrodes, and placed in direct contact with the skin. The entire assembly was secured using a layer of Parafilm to ensure stable contact during physical activity. Wearable measurements were carried out during a controlled physical activity consisting of 20 minutes of cycling. During exercise, sweat passively wetted the microfluidic pad through capillary action, allowing continuous contact between freshly secreted sweat and the sensing electrodes. Potentiometric measurements were started once sufficient wetting of the paper-based microfluidic structure was achieved. The sweat samples collected during wearable measurements (at predefined time points of 7, 14, and 20 minutes) were also analysed using a reference method to assess the accuracy. Prior to sensor placement, the skin was gently rinsed with distilled water and dried to minimise potential contamination. Chloride ion concentration was determined by Mohr titration after the samples were appropriately diluted (1:100 v/v). The titrations were carried out using a 0.02 N silver nitrate solution as the titrant and potassium dichromate as the indicator.

3. Results and discussion

The concept of the device is reported in Fig. 1, which encompasses i) a printed office paper-based electrochemical sensor, in which the working electrode is modified with CB to improve electronic conductivity and then functionalized with a chloride-selective membrane, combined with a pseudo-reference electrode modified with a reference membrane, ii) a paper-based microfluidic system for sweat management during on-body applications, and iii) a wearable wireless potentiostat for real-time data transmission. In the following sections, the optimisation of key fabrication parameters, such as membrane composition, deposition methods, and conditioning protocols, is presented, along with the analytical performances of the sensor in standard solution, artificial sweat, and real sweat collected during physical activity, followed by an on-body test using a wearable device.

3.1. Choice of paper substrate

Unlike conventional polyester supports, paper substrates were selected to ensure a more sustainable, eco-friendly approach, a key aspect in the development of wearable point-of-care devices. Six types of paper were tested and compared for contact angle and analytical performance. Contact angle measurements performed on wax-treated substrates (Fig. S2) showed hydrophobic behaviour for all tested papers ($\theta > 110°$ at $t = 0$ and maintained after 5 min), indicating effective surface modification. Therefore, differences in analytical performance were not attributed to hydrophobicity but rather to substrate structural properties influencing membrane deposition and electrochemical stability. Fig. 2A shows the slope as a function of paper type, indicating that the office paper from Fabriano provided the best overall results. Specifically, it exhibited the highest slope value (55 mV/log a Cl^-), consistent with a Nernstian response, superior repeatability (RSD% = 4.1%), and lower

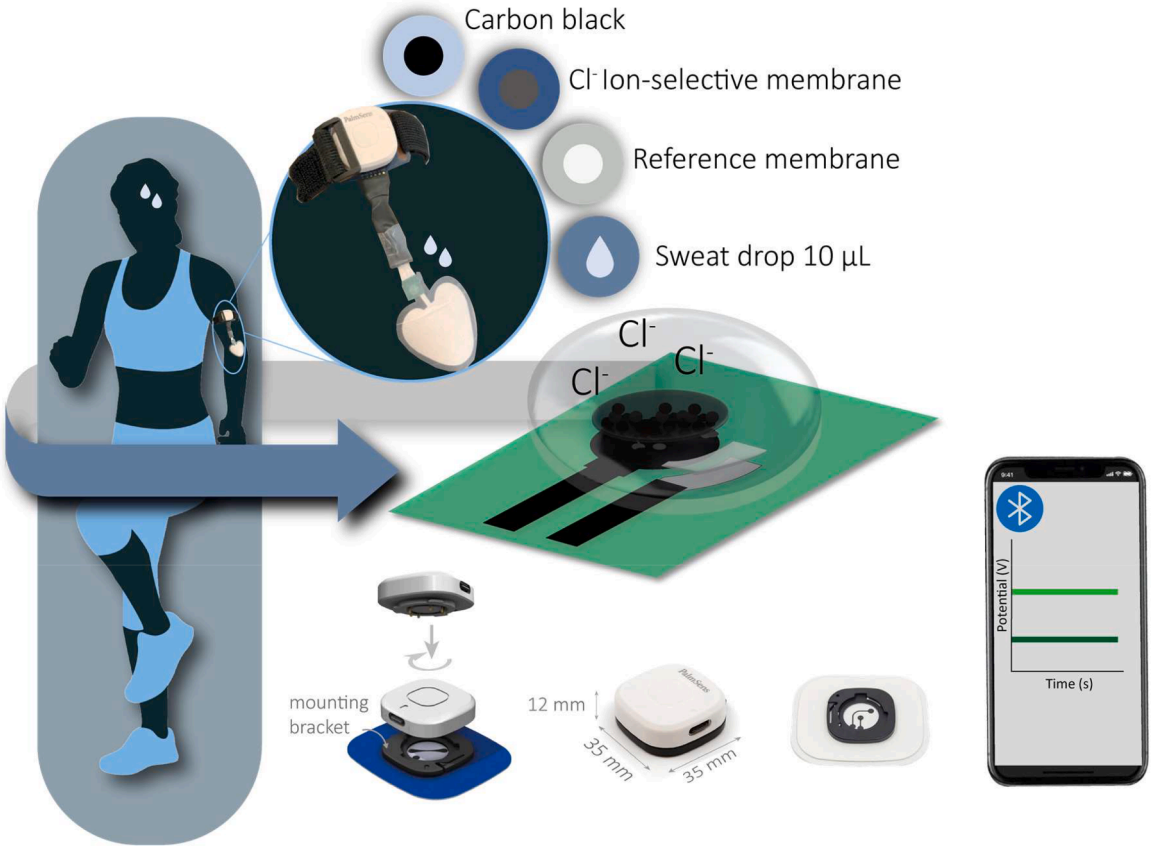

Fig. 1. Schematic illustration of the developed wearable platform for chloride ion detection in sweat.

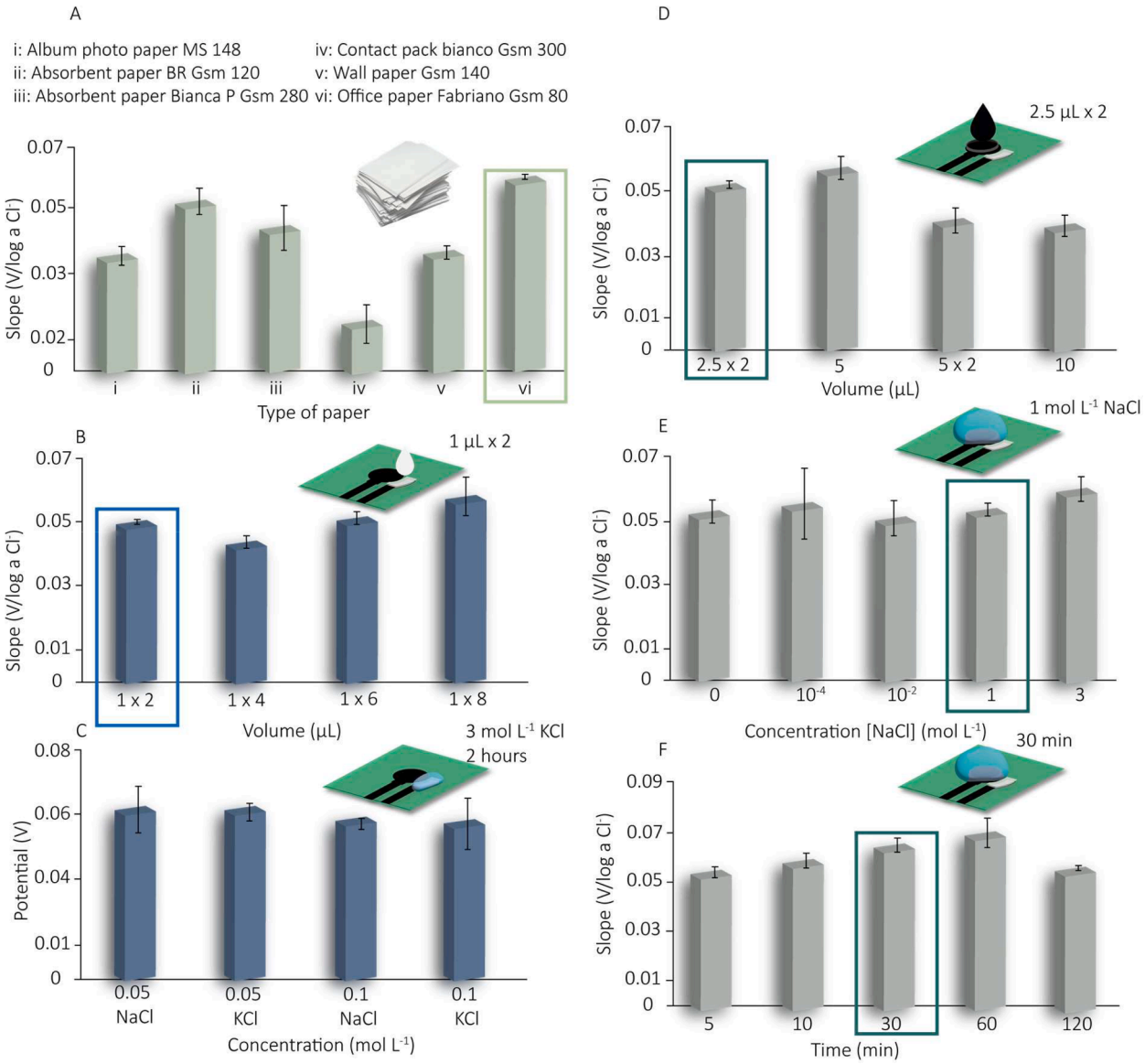

Fig. 2. A) Selection of the optimal paper substrate. B) Optimisation of the reference membrane volume. C) Evaluation of the conditioning time of the reference membrane. D) Selection of the optimal volume for the ion-selective membrane. E) Study of the effect of the conditioning solution concentration on the ion-selective membrane. The response was analysed from no conditioning treatment up to conditioning in 3 mol L^{-1} NaCl. F) Optimisation of the conditioning time for the ion-selective membrane. Conditions highlighted with a coloured box indicate the parameter selected for the final sensor configuration.

material cost than the other tested substrates. Based on these parameters, Fabriano office paper was selected as the most suitable substrate for subsequent sensor fabrication. The improved analytical performance can be attributed to its relatively compact structure and controlled porosity, which favour the formation of a homogeneous and continuous ion-selective membrane during drop-casting. In contrast, more porous substrates, such as filter paper, may partially absorb the membrane solution within the fibrous matrix, potentially affecting film uniformity and phase boundary stability. The more compact surface of office paper supports controlled membrane deposition, contributing to enhanced reproducibility and a slope closer to the ideal Nernstian behaviour. Moreover, this choice is supported by our previous works [20–23], which demonstrates the suitability of office paper for electrochemical applications, even when combined with porous paper-based microfluidics.

3.2. *Optimisation of paper-based printed potentiometric sensor*

To ensure accurate and reliable chloride ion detection, several parameters related to the ion-selective membrane were optimised. The optimisation process involved evaluating the membrane volume deposited onto the electrode surface via drop-casting, the concentration of the conditioning solution, and the conditioning time.

3.2.1. *Reference membrane*

In potentiometric sensors, the reference electrode plays a crucial role in ensuring signal stability and reproducibility, particularly in all-solid-state configurations, where traditional liquid-junction reference systems are replaced by solid materials. The measured potential corresponds to the difference between the working and the reference electrode; therefore, any instability of the reference potential directly affects the analytical signal. To maintain a stable potential, polymer-based reference membranes are commonly doped with a fixed concentration of chloride ions (e.g., NaCl) and subsequently conditioned in concentrated

KCl solutions (typically 3 mol L^{-1}). This approach helps maintain a constant chloride activity at the electrode interface, minimising potential drift and ensuring reproducible measurements in solid-state configurations [24,28]. To ensure reliable performance in real-sample conditions, the reference membrane must provide a stable potential that remains unaffected by variations in ionic strength and sample composition.

The first step of the optimisation involved determining the optimal volume of reference membrane to be cast on the Ag/AgCl pseudo-reference electrode. Volumes ranging from 2 to 8 μL were tested, with each applied in two successive deposition steps to promote uniform membrane formation and prevent material accumulation. As shown in Fig. 2B, a total volume of 2 μL ensured complete and homogeneous coverage of the electrode surface, resulting in the best performance in terms of both sensitivity (49 mV/log a Cl^-) and reproducibility (RSD % = 1.8 %). In contrast, smaller volumes such as 1 μL were insufficient to uniformly coat the electrode, compromising the stability of the electrochemical potential.

Subsequently, the conditioning time of the reference membrane was evaluated. In the literature, long conditioning steps (typically 18 hours in 3 mol L^{-1} KCl solution) are widely reported to promote stable potential development and minimise drift during measurement [24,28]. However, to improve the scalability and reduce the production time of the sensor, a systematic study was conducted to identify the minimum effective conditioning time. The membrane was conditioned in 3 mol L^{-1} KCl for 1, 2, 3, and 18 hours, and the resulting potential stability was assessed (Fig. S3). Notably, a conditioning time of 2 hours was sufficient to achieve a stable and reproducible potential, comparable to that observed after 18 hours, but with a significantly reduced preparation time.

To further verify the effectiveness of the 2-hour conditioning protocol, the pseudo-reference electrode was used as a working electrode, and its potential response was monitored in NaCl and KCl solutions at two different ionic strengths (0.05 mol L^{-1} and 0.1 mol L^{-1}). The recorded potentials showed no significant variation (Fig. 2C), confirming that the electrode was effectively insulated from changes in the ionic composition of the sample, and validating the selected conditioning protocol for practical applications. The use of PVB-based membranes doped with NaCl for pseudo-reference electrodes is widely reported in the literature for paper- and polyester-based potentiometric sensors, as they offer a stable and reproducible potential in miniaturised all-solid-state configurations [28,30,31]. In most cases, these membranes are conditioned for up to 18 hours in concentrated KCl solutions to ensure potential stability; however, in this work, a reduced conditioning time of 2 hours was demonstrated to be equally effective, significantly improving the sensor's production scalability. Moreover, the chloride response of the reference electrode was independently evaluated by using the reference electrode as the working electrode against an external Ag/AgCl reference in different NaCl standard solutions over the range of 1–200 mmol L^{-1}. The results, reported in Fig. S4, show no concentration-dependent potential variation and no Nernstian behaviour (17 mV/log a Cl^-) as expected, confirming the stability and chloride insensitivity of the reference system.

3.2.2. Ion-selective membrane

The ion-selective membrane is a fundamental component of the sensor, as it governs both the selectivity and sensitivity of the sensor toward the target ion. In all-solid-state potentiometric sensors, the membrane must form a homogeneous and stable film over the transducing layer, ensuring efficient ion-exchange dynamics and minimal signal drift. To this end, three critical parameters were optimised, namely the membrane volume cast, the concentration of the conditioning solution, and the conditioning time.

Different ion-selective membrane volumes were tested to determine the optimal thickness that ensures both mechanical stability and electrochemical responsiveness. In detail, 5 μL and 10 μL were cast in a single step, as well as split applications of 5 μL (2 × 2.5 μL) and 10 μL (2 × 5 μL). As shown in Fig. 2D, the deposition of 5 μL in two steps of 2.5 μL led to improved repeatability (RSD %= 8.36 %) and yielded a slope closer to the ideal Nernstian behaviour (50 mV/log a Cl^-) for monovalent anions, indicating enhanced electrochemical performance and more stable membrane formation. The use of an ion-selective membrane with a volume of 2.5 μL did not allow the formation of a homogeneous film on the working electrode surface.

Following membrane deposition, the conditioning step was optimised to promote ion exchange at the membrane/electrolyte interface and to stabilise the membrane potential. To this end, NaCl conditioning solutions of increasing concentration, ranging from 0 to 3 mol L^{-1}, were tested. As illustrated in Fig. 2E, a concentration of 1 mol L^{-1} NaCl provided the best compromise between slope linearity and signal repeatability, making it the most suitable choice for membrane pretreatment.

Finally, different conditioning times were tested, ranging from 5 to 120 minutes. A conditioning time of 30 minutes was selected as the minimum time required to achieve both the desired Nernstian response and high measurement repeatability (Fig. 2F), without unnecessarily extending the sensor preparation process. Similar conditioning strategies based on short-term exposure to monovalent ion solutions have been reported for ion-selective membranes in solid-contact sensors [26,30], supporting the feasibility of reducing preparation times without compromising sensor stability.

3.3. Analytical characterisation

After optimising the fabrication and conditioning parameters, the analytical performances of the chloride-selective sensor were evaluated under standard conditions. A calibration curve was obtained by measuring NaCl standard solutions over a concentration range of 1 to 200 mmol L^{-1}. The sensor exhibited good linearity within the tested range, as described by the equation $y = (-0.051 \pm 0.002)\,x + (0.214 \pm 0.004)$, with a correlation coefficient $R^2 = 0.978$ (Fig. 3A). Calibration curves were obtained using three independently fabricated sensors (n = 3). Linear regression was performed using SigmaPlot software, and the reported uncertainties correspond to the standard errors of the fit. These results confirmed the sensor's capability to provide a reliable and reproducible potentiometric response, exhibiting near-Nernstian behaviour. The repeatability of the sensor was assessed by evaluating the potential response at 10 mmol L^{-1} NaCl in triplicate. The resulting relative standard deviation (RSD %) was 0.65 %, highlighting the high precision and manufacturing consistency of the sensor platform. The limit of detection (LOD) was calculated as the intersection of the two slope lines and was found to be equal to 70 μmol L^{-1}. This value is competitive with values reported in the state of the art for chloride ion sensors in sweat (Table 1), thanks to the optimised conditions and the use of CB, demonstrating that reliable and highly sensitive chloride ion detection is achieved even with a simple fabrication strategy and eco-friendly materials were selected.

Given the intended application of the device in a wearable and continuous monitoring system, the signal drift over time was also examined. A 2-hour open-circuit potentiometric measurement was carried out in a 200 mmol L^{-1} NaCl solution, obtaining a drift equal to 4.1 mV h^{-1} (Fig. 3B). Furthermore, to investigate the possible occurrence of memory effects, a hysteresis study was performed by exposing the same sensor to a sequence of NaCl solutions with increasing and then decreasing concentrations, ranging from 1 to 200 mmol L^{-1}. In addition, a water-layer test was carried out to evaluate the possible formation of an aqueous film at the interface between the electrode surface and the ion-selective membrane (Fig. S5). A significant potential drift was observed when switching between NaCl and $NaNO_3$ solutions using the bare SPE, indicating the formation of an interfacial water layer. In contrast, the CB-modified electrode exhibited a stable potential response with negligible drift, confirming the absence of a water layer. This behaviour can be attributed to the hydrophobic nature of CB, which

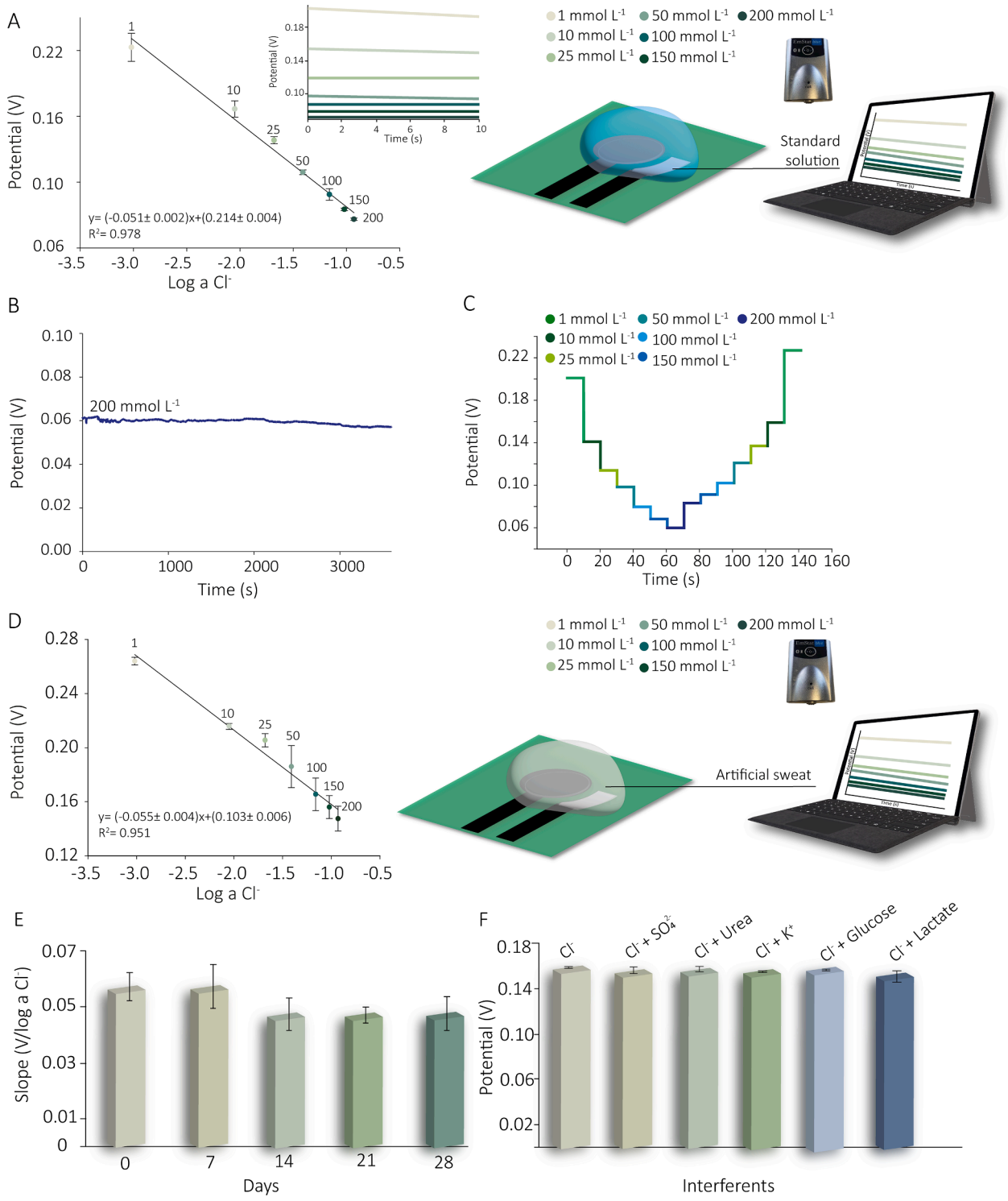

Fig. 3. A) Calibration curve and potentiograms (inset) obtained using CB-SPEs modified with 5 µL of ion-selective membrane mixture and 2 µL of reference membrane, measuring 50 µL of a solution containing Cl^- 1, 10, 25, 50, 100, 150, and 200 mmol L^{-1}. B) Working stability study obtained by measuring 200 mmol L^{-1} NaCl for 2 hours using CB-modified SPE. Ion-selective membrane: 5 µL, reference membrane: 2 µL. C) Hysteresis study for the Cl^- sensor measuring 50 µL of chloride ion standard solution in the range of 1–200 mmol L^{-1} and vice versa. D) Calibration curve obtained using CB-SPEs modified with 5 µL of mixture for ion-selective membrane and 2 µL of reference membrane, measuring 50 µL of an artificial sweat containing chloride ions 1, 10, 25, 50, 100, 150, and 200 mmol L^{-1}. E) Slope of calibration curves obtained with standard solution of NaCl at concentrations 1, 10, 25, 50, 100, 150, and 200 mmol L^{-1} on the same day of the ion-selective and reference membrane deposition, and after 7, 14, 21, and 28 days. F) Histogram obtained for the detection of 10 mmol L^{-1} Cl^- in the presence of 0.25 mol L^{-1} sulphate, 3 mmol L^{-1} urea, 6 mmol L^{-1} potassium, 0.3 mmol L^{-1} glucose, and 25 mmol L^{-1} lactate.

Table 1
Comparison of (electrochemical) sensors for chloride ion detection in sweat.

Type of sensor	Technique	Sensing material	Modification procedure	Linear range	Slope	LOD	Microfluidics	Hysteresis study with micro-fluidics	Wearable	Matrix	Ref
Thin-film sensor	Potentio-metry	Ag/AgCl	-	10-150 mmol L^{-1}	58.5 mV/ log c Cl^-	-	- *	-	yes	Human sweat	[13]
Textile-based sensor	Potentio-metry	Chloride Ion-selective membrane	Drop-casting	0.1–100 mmol L^{-1}	59.5 mV/ log c Cl^-	-	A super-absorbent fiber was attached to the sensor cloth to continuously remove the old sweat from the sensing part of the sensor	-	yes	Human sweat	[16]
Thin-film gold electrode	Chrono-amperometry	Ag nanoparticles	Electrodeposition	1-100 mmol L^{-1}	1.44 μA/ mmol L^{-1}	39 μmol L^{-1}	Paper-based microfluidics device (Whatman cellulose chromatographic paper, Grade 1)	-	-	Artificial sweat	[17]
SPE	Potentio-metry	Ion-selective membrane (Chloride Ionophore I-Cocktail A)	Drop-casting	0.1-100 mmol L^{-1}	62.9 mV/ log c Cl^-	27 μmol L^{-1}	-	-	-	Human sweat	[25]
Chemosensor	Colo-rimetric	Hydrogel (BC–CMC–Ch) on PDMS	-	20-100 mmol L^{-1}	-	560 μmol L^{-1}	PDMS-based microfluidics	-	yes	Artificial sweat	[34]
SPCE	Linear Scan Voltammetry	Ag nanoparticles	Electrodeposition	5-60 mmol L^{-1}	2.92 μA/ mmol L^{-1}	-	-	-	-	Synthetic sweat	[35]
SPE	Cyclic Voltammetry	Ag nanoparticles	Drop-casting	2-40 mmol L^{-1}	-	-	-	-	-	1:4 v/v diluted synthetic sweat	[36]
Paper-based SPE	Cyclic Voltammetry	Ag ink	H_2SO_4 drop-casting	10-200 mmol L^{-1}	1.98 μA/ mmol L^{-1}	1000 μmol L^{-1}	-	-	-	Human sweat and serum	[37]
Paper-based wearable sensor	Potentio-metry	Ion-selective membrane (Chloride Ionophore I-Cocktail A)	Drop-casting	1-200 mmol L^{-1}	51 mV/ log a Cl^- in buffer, 56 mV/ log a Cl^- in artificial sweat	70 μmol L^{-1} in buffer, 74 μmol L^{-1} in artificial sweat	Fully paper-based microfluidic interface featuring an apple-like geometry, which passively guides fresh sweat over the sensing area	yes, demonstrating no memory effect	yes	Human sweat	Our work

• the working electrode is formed on the bottom side of the PET film and directly contacts the skin, ** cotton textile-thread sensor added in an artificial sweat solution.
SPE= Screen-printed electrode; BC= Bacterial cellulose; CMC= Carboxymethyl cellulose; Ch= Chitosan; PDMS= Polydimethylsiloxane; SPCE= Screen-printed carbon electrode.

prevents water accumulation at the electrode–membrane interface and contributes to the improved stability of the potentiometric signal. As shown in Fig. 3C, a noticeable difference was observed between the forward and reverse calibration curves, indicating the presence of a non-negligible memory effect under static measurement conditions. This behaviour can be attributed to partial retention of the previously analysed sample at the electrode surface, which may affect the sensor response when consecutive measurements are performed without continuous sample renewal. Although this effect does not compromise the analytical performances under single-use or static conditions, it highlights a limitation for real-time and continuous monitoring applications, which is effectively addressed through the integration of the paper-based microfluidic system described in the following section.

Subsequently, to evaluate the sensor's performance in physiologically relevant conditions, a calibration curve was obtained in artificial sweat. The artificial matrix was prepared as described in Section 2.8, containing the main ionic and organic constituents of human sweat at physiological concentrations. As shown in Fig. 3D, the device exhibited a linear response over the range of 1 to 200 mmol L^{-1} chloride ions, with a regression equation of $y = (-0.055 \pm 0.004)\ x + (0.103 \pm 0.006)$, correlation coefficient (R^2) of 0.951, and LOD equal to 74 μmol L^{-1}, which is very close to the value obtained in standard solutions (70 μmol L^{-1}). These results confirm the sensor's ability to function effectively in complex matrices, maintaining a near-Nernstian behaviour even in the presence of common sweat interferents. The storage stability of the sensor was also evaluated. The devices were stored under vacuum at room temperature and tested weekly for a period of four weeks. As shown in Fig. 3E, the slope of the calibration curve decreased by 17.24 % after two weeks but then remained stable up to 28 days. This result demonstrates a good long-term stability profile, making the sensor suitable for short- to medium-term storage without requiring special preservation conditions.

Finally, a selectivity study was conducted to assess potential interference from common constituents of sweat. Sulphate ions, urea, potassium ions, glucose, and lactate were tested individually at their physiological concentrations in sweat. As shown in Fig. 3F, none of these interfering species produced significant deviations in the potential response to chloride, thus confirming the high selectivity of the sensor toward chloride ions. In addition, potentiometric selectivity coefficients (log K^{pot}) were calculated using the Two Solution Method (TSM). The obtained values were $\log K^{pot}_{Cl^-,SO_4^{2-}} = -1.36$ and $\log K^{pot}_{Cl^-,Lactate} = -1.30$, indicating limited interference from representative sweat anions. The response toward K^+ was negligible ($\log K^{pot}_{Cl^-,K^+} = -6.89$), further confirming the specificity of the ion-selective membrane. Finally, to further investigate the electrochemical properties of the sensing interface, Electrochemical Impedance Spectroscopy (EIS) measurements were performed on sensors with and without the CB modification layer (Fig. S1). As expected, the introduction of CB significantly improved the low-frequency capacitance (50.7 μF, f = 0.01 Hz) with respect to the bare electrode (26.9 μF, f = 0.01 Hz), confirming the enhanced and stabilised ion-to-electron transduction capability due to the double-layer capacitive mechanism of CB, as previously reported in the literature [27].

3.4. Sweat analysis

3.4.1. Apple-like paper-based microfluidic device

Inspired by the work of Pradela-Filho et al. [32], which demonstrated that expanding outlet geometries such as fan-shaped or radial paper reservoirs can significantly improve fluid handling and enable quasi-steady continuous flow in electrochemical paper-based devices, an *apple-like* paper-based microfluidic interface was designed, fabricated, and integrated into the sensing platform. The device was fabricated via CO_2 laser cutting on filter paper, creating a passive and capillary-driven flow path without the need for an external pump.

The geometry was developed by modifying the butterfly-shaped configuration previously proposed by Fiore et al. [30], which was originally designed for multi-analyte sensing. In the present work, the layout was tailored for single-analyte detection and adapted to a compact *apple-like* design. This configuration allows for an enlarged waste zone, enhancing sweat management, and ensuring a unidirectional flow of freshly secreted sweat over the sensing electrodes, while directing the analysed sample away from the detection zone. This design minimises memory effects and enables real-time monitoring of both increases and decreases in sweat chloride ion concentration, e.g., during phases of dehydration and rehydration in prolonged exercise.

The device is composed of two main regions: a sampling zone, positioned directly over the skin to collect sweat during physical activity, and a waste zone, which passively absorbs the analysed fluid. The two areas are connected by a narrow channel that guides the flow via capillary forces, eliminating the need for external pumps or power sources.

The microfluidic layer was simply placed onto the electrode surface, aligning the sampling zone with the working and reference areas of the sensor. This flow-through architecture, inspired by previously reported capillary-expanding geometries, ensures continuous fluid replacement at the electrode surface, prevents evaporation, and maintains measurement accuracy over time. As such, this simple yet efficient device provides a reliable and scalable solution for on-body chloride ion monitoring, representing a key advancement over previously reported wearable microfluidic sensors (Table 1).

3.4.2. Integrated wearable sensor for chloride ions quantification in artificial and real sweat

After validating the sensor's analytical performances under both standard and artificial sweat conditions, the complete wearable configuration was tested by integrating the chloride-selective sensor with the previously described paper-based microfluidic device. The integrated system was first evaluated using a benchtop potentiostat to characterise its behaviour in artificial sweat under dynamic flow conditions. As shown in Fig. 4A, the device exhibited a linear response in the range 1-200 mmol L^{-1}, a sensitivity of 56 ± 2 mV/log a Cl^-, and LOD equal to 74 μmol L^{-1}, demonstrating that the addition of the microfluidic interface did not compromise the electrochemical performance of the sensor in complex matrices. The signal drift under these conditions was then evaluated using the same microfluidic-paper configuration. As shown in Fig. 4B, the device exhibited a drift of 3.8 mV h^{-1}, which is lower than the 4.1 mV h^{-1} observed when the sensor was used without the microfluidic layer. This improvement can be attributed to the capillary-driven flow enabled by the microfluidic structure, which allows continuous sample renewal at the electrode surface, reducing the impact of evaporation and accumulation.

The observed drift was comparable to values reported in other similar works. For instance, Gao et al. [26] reported drift values of 2–3 mV h^{-1} in wearable platforms using liquid-contact reference electrodes on plastic substrates, while Tseng et al. [33] observed drift rates between 2.5 and 8.2 mV h^{-1} for flexible RuO_2-GO chloride sensors in a paperless arrayed configuration.

The reduced drift observed in our all-paper system likely reflects the combined effect of optimised membrane deposition, short conditioning time, and the use of a stable solid-state reference electrode, confirming the sensor's suitability for real-time, on-body chloride ion monitoring. To assess the influence of the microfluidic component on measurement stability, a hysteresis test was performed by measuring a series of chloride ion concentrations in both ascending and descending orders. As shown in Fig. 4C, the sensor did not exhibit any significant memory effect when combined with the microfluidic layer, in contrast to the results obtained without microfluidics, likely due to residual sample accumulation at the sensing interface. The inclusion of the waste zone in the *apple-like* geometry ensured the continuous removal of the analysed sample, thus preventing memory effects and enabling the accurate tracking of both increasing and decreasing chloride ion levels during

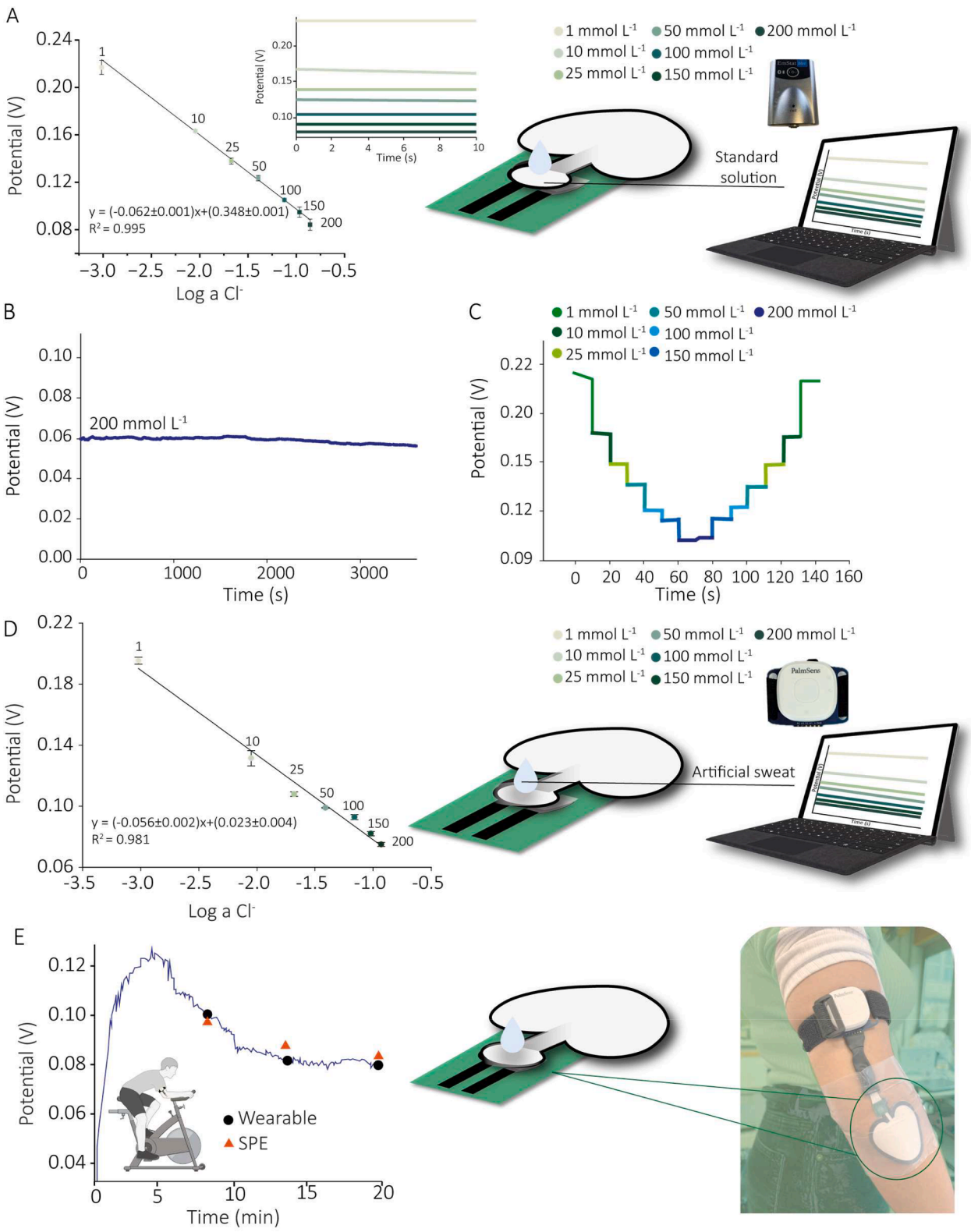

Fig. 4. A) Calibration curve obtained using apple-like paper-based sensor modified with 5 µL of a mixture for ion-selective membrane and 2 µL of reference membrane and paper-based microfluidic pad measuring 10 µL of a standard solution containing Cl^- 1, 10, 25, 50, 100, 150 and 200 mmol L^{-1}. B) Working stability study obtained by measuring 200 mmol L^{-1} NaCl for 2 hours using an apple-like paper-based sensor. Ion-selective membrane: 5 µL, reference membrane: 2 µL, and paper pad microfluidics. C) Hysteresis study for the Cl^- sensor measuring 10 µL of chloride ion standard solution in the range of 1–200 mmol L^{-1} and vice versa. D) Calibration curve obtained using an apple-like wearable sensor modified with 5 µL of mixture for ion-selective membrane and 2 µL of reference membrane and paper pad microfluidics measuring 10 µL of an artificial sweat solution containing Cl^- 1, 10, 25, 50, 100, 150, and 200 mmol L^{-1}. E) The chloride ion concentration was continuously recorded in real time throughout a 20-minute stationary cycling session, with data wirelessly transmitted via Bluetooth to a connected device. Discrete chloride iconcentrations obtained after 7, 14, and 20 minutes of exercise from the wearable continuous measurement were compared with point measurements performed using an *apple-like* wearable sensor and with the reference method.

prolonged exercise or hydration cycles, which goes beyond the state of the art, as highlighted in Table 1. Subsequently, to simulate realistic wearable operation, the complete system, comprising the chloride-selective sensor, paper-based microfluidic interface, and the Sensit/Wearable potentiostat, was used to obtain a calibration curve in artificial sweat, as shown in Fig. 4D. The resulting response was comparable to that obtained with the benchtop potentiostat, confirming that neither the microfluidic integration nor the portable electronics negatively affect sensor performance, and that the proposed platform is well-suited for wearable and real-time monitoring of sweat composition. Finally, to further validate the functionality of the complete wearable system under real conditions, the device was tested *in vivo* during physical activity. A healthy volunteer wore the sensor integrated with the paper-based microfluidic system and the Sensit/Wearable potentiostat while performing a 20-minute cycling session. The sensor continuously recorded the chloride ion concentration in real time throughout the exercise, with data transmitted wirelessly to a connected device.

As illustrated in Fig. 4E, an initial lag phase was observed during the first few minutes of exercise (~5 minutes), corresponding to the time required for sweat to reach and sufficiently wet the sensing area, enabling a stable electrochemical response. Following this, the sensor began to detect chloride ion levels in sweat, which show a progressive increase over time. This trend is consistent with the dynamics of sweat composition during prolonged physical activity, where increased sweating and dehydration result in a higher concentration of chloride ions in the collected sweat.

To test the accuracy of the continuous monitoring data, three discrete sweat samples were also analysed at 7, 14, and 20 minutes using both the developed screen-printed sensor (at a point-of-care set-up) and the reference Mohr titration method. The corresponding chloride ion concentrations are reported in Table 2. As shown in Fig. 4E, the chloride ion concentrations measured at these time points closely match the trend observed in the continuous recording. The agreement between the wearable, screen-printed, and the reference method confirms the accuracy of the proposed sensing system for real-time sweat chloride ion analysis in wearable applications.

To contextualise the analytical performances of the developed chloride sensor, a comparison was made with previously reported potentiometric and amperometric devices for chloride ion detection in sweat (Table 1). Key performance indicators such as linear range, slope, LOD, and integration into wearable formats were considered. The proposed sensor exhibits a broad linear range of 1–200 mmol L^{-1}, effectively covering both physiological and pathological levels of chloride ions in sweat, which is particularly relevant for the diagnosis and monitoring of cystic fibrosis, ensuring applicability for both healthy individuals and patients with elevated sweat chloride ion levels. Furthermore, the combination of the paper-based sensor with a fully paper-based microfluidic interface featuring an *apple-like* geometry enables the flow of fresh sweat over the sensing area and directs the analysed sample toward a waste zone without any memory effect. This continuous-flow design prevents sweat accumulation and evaporation, supporting stable and accurate detection over time. Unlike static or closed systems, this configuration enables the dynamic monitoring of physiological changes, such as increases in chloride ion concentration due to dehydration or decreases following rehydration during prolonged exercise. The effectiveness of this approach was confirmed by hysteresis analysis, while a memory effect was observed under static conditions, no hysteresis was detected when the microfluidic component was applied. In this configuration, regeneration was inherently achieved through continuous capillary-driven transport of the sample toward the waste zone, ensuring effective removal of the previously analysed solution and continuous renewal at the sensing interface, thus validating its role in enabling accurate sensor response during continuous on-body monitoring.

Table 2
Detection of chloride ion concentrations of three sweat samples by using the *apple-like* wearable sensor and the reference Mohr titration method.

Sample sweat	Reference method (mmol L^{-1})	Electrochemical sensor (mmol L^{-1})	Relative Error
1	77	66	-14%
2	70	64	-9%
3	95	99	4%

4. Conclusions

Herein, a fully solid-state, paper-based potentiometric sensor was developed, optimised, and tested for the selective detection of chloride ions in human sweat. The sensor was fabricated on office paper using wax patterning and screen-printing of graphite and Ag/AgCl inks to define the working and pseudo-reference electrodes. The working electrode was further modified with CB to improve electronic conductivity and then functionalized with a chloride-selective membrane. Meanwhile, the pseudo-reference electrode was stabilised through the deposition and conditioning of a dedicated reference membrane. In addition to the electrochemical platform, a paper-based microfluidic device was designed and integrated with the sensor to enable continuous, passive sweat flow during on-body applications. The paper-based device integrated with a wearable wireless potentiostat allowed for real-time data transmission and autonomous operation in practical settings by quantifying chloride ions up to 200 mmol L^{-1} with a detection limit of 74 μmol L^{-1} and a sensitivity of 56 mV/log a Cl^-. The reliable design based on a combination of a chloride-selective membrane with an office paper-based screen-printed solid-contact electrode and a capillary-driven microfluidic network ensured effective sample delivery and memory-free analyses. The data obtained in on-body measurements were found to agree with the standard method, demonstrating the accuracy of this fully paper-based wearable platform for non-invasive electrolyte monitoring, with potential applications in cystic fibrosis diagnostics and broader physiological monitoring.

Ethical approval

Experiments involving human subjects have been approved by the local ethical committee (Italian Army Medical Hospital, Rome), which gave a favorable ethical opinion based on the document CE/202lu/03/a-31/03/2021–09.b, in the study project “SAlute e BEnessere dei VETerani” (“SA.BE.VET”).

Funding

This study was supported by Patchstress project, Italian Ministry of Defence and PRIN2022 project SMARTMASK4CF.

CRediT authorship contribution statement

Luca Fiore: Writing – original draft, Visualization, Methodology, Investigation, Formal analysis, Data curation, Conceptualization. **Giorgia Leotta:** Visualization, Formal analysis, Data curation. **Matteo di Carmine:** Formal analysis, Data curation. **Arianna Antinucci:** Formal analysis. **Florigio Lista:** Writing – review & editing, Project administration, Funding acquisition. **Fabiana Arduini:** Writing – review & editing, Writing – original draft, Supervision, Resources, Project administration, Funding acquisition, Conceptualization.

Declaration of competing interest

The authors declare that they have no known competing financial interests or personal relationships that could have appeared to influence the work reported in this paper.

Supplementary materials

Supplementary material associated with this article can be found, in the online version, at doi:10.1016/j.electacta.2026.148692.

Data availability

Data will be made available on request.

References

[1] World Economic Forum, Top emerging technologies report of 2017. https://www3.weforum.org/docs/WEF_Top_10_Emerging_Technologies_report_2017.pdf, 2017 (accessed on 8 January 2026).

[2] N. Brasier, J. Wang, W. Gao, J.R. Sempionatto, C. Dincer, H.C. Ates, F. Güder, S. Olenik, I. Schauwecker, D. Schaffarczyk, E. Vayena, N. Ritz, M. Weisser, S. Mtenga, R. Ghaffari, J.A. Rogers, J. Goldhahn, Applied body-fluid analysis by wearable devices, Nature 636 (2024) 57–68, https://doi.org/10.1038/s41586-024-08249-4.

[3] N. Traeger, Q. Shi, A.J. Dozor, Relationship between sweat chloride, sodium, and age in clinically obtained samples, J. Cyst. Fibros. 13 (2014) 10–14, https://doi.org/10.1016/j.jcf.2013.07.003.

[4] P.M. Farrell, T.B. White, C.L. Ren, S.E. Hempstead, F. Accurso, N. Derichs, M. Howenstine, S.A. McColley, M. Rock, M. Rosenfeld, I. Sermet-Gaudelus, K. W. Southern, B.C. Marshall, P.R. Sosnay, Diagnosis of cystic fibrosis: consensus guidelines from the cystic fibrosis foundation, J. Pediatr. 181 (2017) S4–S15.e1, https://doi.org/10.1016/j.jpeds.2016.09.064.

[5] P.M. Farrell, T.B. White, Introduction to Cystic Fibrosis Foundation consensus guidelines for diagnosis of cystic fibrosis, J. Pediatr. 181 (2017) S1–S3, https://doi.org/10.1016/j.jpeds.2016.09.062.

[6] Association for Clinical Biochemistry, Guidelines for the Performance of the Sweat Test for the investigation of cystic fibrosis in the UK. http://www.acb.org.uk/, 2003 (accessed on 8 January 2026).

[7] D.H. Choi, G.B. Kitchen, K.J. Stewart, P.C. Searson, The dynamic response of sweat chloride to changes in exercise load measured by a wearable sweat sensor, Sci. Rep. 10 (2020) 7699, https://doi.org/10.1038/s41598-020-64406-5.

[8] L.B. Baker, A.S. Wolfe, Physiological mechanisms determining eccrine sweat composition, Eur J. Appl. Physiol. 120 (2020) 719–752, https://doi.org/10.1007/s00421-020-04323-7.

[9] B.J. Rosenstein, G.R. Cutting, The diagnosis of cystic fibrosis: A consensus statement, J. Pediatr. 132 (1998) 589–595, https://doi.org/10.1016/S0022-3476(98)70344-0.

[10] N. Cirilli, K.W. Southern, J. Barben, F. Vermeulen, A. Munck, M. Wilschanski, T. Nguyen-Khoa, M. Aralica, N. Simmonds, E. De Wachter, Standards of care guidance for sweat testing; phase two of the ECFS quality improvement programme, J. Cyst. Fibros. 21 (2022) 434–441, https://doi.org/10.1016/j.jcf.2022.01.004.

[11] D.R. VanDevanter, M.W. Konstan, Outcome measures for clinical trials assessing treatment of cystic fibrosis lung disease, J. Clin. Invest. 2 (2012) 163–175, https://doi.org/10.4155/cli.11.174.

[12] E.T. Zemanick, M.W. Konstan, D.R. VanDevanter, S.M. Rowe, J. Clancy, K. Odem-Davis, M. Skalland, N. Mayer-Hamblett, Measuring the impact of CFTR modulation on sweat chloride in cystic fibrosis: Rationale and design of the CHEC-SC study, J. Cyst. Fibros. 20 (2021) 965–971, https://doi.org/10.1016/j.jcf.2021.01.011.

[13] D.H. Choi, Y. Li, G.R. Cutting, P.C. Searson, A wearable potentiometric sensor with integrated salt bridge for sweat chloride measurement, Sens. Actuators B Chem. 250 (2017) 673–678, https://doi.org/10.1016/j.snb.2017.04.129.

[14] C.-L. Wang, X. Cai, Y.-H. Zhao, Z.-H. Liu, R.-Z. Xia, L.-J. Tang, Z.-Y. Song, S.-H. Chen, Y. Li, M. Yang, P.-H. Li, X.-J. Huang, Integrated headband for monitoring chloride anions in sweat using developed flexible patches, ACS Sens 10 (2025) 3441–3449, https://doi.org/10.1021/acssensors.4c03366.

[15] F. Arduini, Paper as a sustainable material for smart electrochemical (bio)sensors with unprecedented features: A perspective, Anal. Chem. 97 (2025) 10126–10138, https://doi.org/10.1021/acs.analchem.5c00128.

[16] I. Shitanda, N. Muramatsu, R. Kimura, N. Takahashi, K. Watanabe, H. Matsui, N. Loew, M. Motosuke, T. Mukaimoto, M. Kobayashi, T. Mitsuhara, Y. Sugita, K. Matsuo, S. Yanagita, T. Suzuki, H. Watanabe, M. Itagaki, Wearable ion sensors for the detection of sweat ions fabricated by heat-transfer printing, ACS Sens 8 (2023) 2889–2895, https://doi.org/10.1021/acssensors.3c01027.

[17] M.G. Bruno, M. Gutiérrez-Capitán, B. Patella, G. Aiello, R. Inguanta, C. Fernández-Sánchez, Paper-based microfluidic electrochemical sensor for chloride ion and uric acid detection in sweat, Talanta 298 (2026) 128969, https://doi.org/10.1016/j.talanta.2025.128969.

[18] K. Phoonsawat, T. Ozer, W. Dungchai, C.S. Henry, Dual-mode ion-selective electrodes and distance-based microfluidic device for detection of multiple urinary electrolytes, Analyst 147 (2022) 4517–4524, https://doi.org/10.1039/D2AN01220K.

[19] K. Phoonsawat, I. Agir, W. Dungchai, T. Ozer, C.S. Henry, A smartphone-assisted hybrid sensor for simultaneous potentiometric and distance-based detection of electrolytes, Analytica Chimica Acta 1226 (2022) 340245, https://doi.org/10.1016/j.aca.2022.340245.

[20] S. Cinti, B. De Lellis, D. Moscone, F. Arduini, Sustainable monitoring of Zn(II) in biological fluids using office paper, Sens. Actuators B Chem. 253 (2017) 1199–1206, https://doi.org/10.1016/j.snb.2017.07.161.

[21] F. Arduini, S. Cinti, V. Caratelli, L. Amendola, G. Palleschi, D. Moscone, Origami multiple paper-based electrochemical biosensors for pesticide detection, Biosens. Bioelectron. 126 (2019) 346–354, https://doi.org/10.1016/j.bios.2018.10.014.

[22] S. Cinti, M. Basso, D. Moscone, F. Arduini, A paper-based nanomodified electrochemical biosensor for ethanol detection in beers, Anal. Chim. Acta 960 (2017) 123–130, https://doi.org/10.1016/j.aca.2017.01.010.

[23] V. Caratelli, S. Fillo, N. D'Amore, O. Rossetto, M. Pirazzini, M. Moccia, C. Avitabile, D. Moscone, F. Lista, F. Arduini, Paper-based electrochemical peptide sensor for on-site detection of botulinum neurotoxin serotype A and C, Biosens. Bioelectron. 183 (2021) 113210, https://doi.org/10.1016/j.bios.2021.113210.

[24] V. Mazzaracchio, A. Serani, L. Fiore, D. Moscone, F. Arduini, All-solid state ion-selective carbon black-modified printed electrode for sodium detection in sweat, Electrochim. Acta 394 (2021) 139050, https://doi.org/10.1016/j.electacta.2021.139050.

[25] A. Hauke, S. Oertel, L. Knoke, V. Fein, C. Maier, F. Brinkmann, M.P.M. Jank, Screen-Printed Sensor for low-cost chloride analysis in sweat for rapid diagnosis and monitoring of cystic fibrosis, Biosensors 10 (2020) 123, https://doi.org/10.3390/bios10090123.

[26] W. Gao, S. Emaminejad, H.Y.Y. Nyein, S. Challa, K. Chen, A. Peck, H.M. Fahad, H. Ota, H. Shiraki, D. Kiriya, D.-H. Lien, G.A. Brooks, R.W. Davis, A. Javey, Fully integrated wearable sensor arrays for multiplexed in situ perspiration analysis, Nature 529 (2016) 509–514, https://doi.org/10.1038/nature16521.

[27] C. Gosti, Z. Mousavi, L. Fiore, V. Mazzaracchio, F. Olivieri, G. Gentile, F. Arduini, J. Bobacka, Carbon black and PEDOT:PSS in a synergistic solid contact for reliable printed potentiometric sensors, ACS Sens 10 (2025) 7820–7831, https://doi.org/10.1021/acssensors.5c02226.

[28] T. Guinovart, G.A. Crespo, F.X. Rius, F.J. Andrade, A reference electrode based on polyvinyl butyral (PVB) polymer for decentralized chemical measurements, Anal. Chim. Acta 821 (2014) 72–80, https://doi.org/10.1016/j.aca.2014.02.028.

[29] Z. Zhang, Z. Li, K. Wei, Z. Cao, Z. Zhu, R. Chen, Sweat as a source of non-invasive biomarkers for clinical diagnosis: An overview, Talanta 273 (2024) 125865, https://doi.org/10.1016/j.talanta.2024.125865.

[30] L. Fiore, V. Mazzaracchio, A. Antinucci, R. Ferrara, T. Sciarra, F. Lista, A.Q. Shen, F. Arduini, Wearable electrochemical device based on butterfly-like paper-based microfluidics for pH and Na^+ monitoring in sweat, Microchim. Acta 191 (2024) 580, https://doi.org/10.1007/s00604-024-06564-1.

[31] J.H. Jin, J. Kim, S. Lee, S. Choi, C. Park, N. Min, A Fully Integrated Paper-Microfluidic Electrochemical device for simultaneous analysis of physiologic blood ions, Sensors 18 (2018) 104, https://doi.org/10.3390/s18010104.

[32] L.A. Pradela-Filho, E. Noviana, D.A.G. Araújo, R.M. Takeuchi, A.L. Santos, C. S. Henry, Rapid analysis in continuous-flow electrochemical paper-based analytical devices, ACS Sens 5 (2020) 274–281, https://doi.org/10.1021/acssensors.9b02298.

[33] S.-C. Tseng, T.-Y. Wu, J.-C. Chou, Y.-H. Liao, C.-H. Lai, S.-J. Yan, T.-W. Tseng, Investigation of sensitivities and drift effects of the arrayed flexible chloride sensor based on RuO_2/GO at different temperatures, Sensors 18 (2018) 632, https://doi.org/10.3390/s18020632.

[34] Y.T. Tai, C.Y. Wei, F.H. Ko, Hydrogel-based colorimetric power-saving sensors for on-site detection of chloride ions and glucose in sweat, Biosens. Bioelectron. 271 (2025) 117041, https://doi.org/10.1016/j.bios.2024.117041.

[35] J. Bujes-Garrido, D. Izquierdo-Bote, A. Heras, A. Colina, M.J. Arcos-Martínez, Determination of halides using Ag nanoparticles-modified disposable electrodes. A first approach to a wearable sensor for quantification of chloride ions, Anal. Chim. Acta 1012 (2018) 42–48, https://doi.org/10.1016/j.aca.2018.01.063.

[36] H.S. Toh, C. Batchelor-McAuley, K. Tschulik, R.G. Compton, Electrochemical detection of chloride levels in sweat using silver nanoparticles: a basis for the preliminary screening for cystic fibrosis, Analyst 138 (2013) 4292, https://doi.org/10.1039/c3an00843f.

[37] S. Cinti, L. Fiore, R. Massoud, C. Cortese, D. Moscone, G. Palleschi, F. Arduini, Low-cost and reagent-free paper-based device to detect chloride ions in serum and sweat, Talanta 179 (2018) 186–192, https://doi.org/10.1016/j.talanta.2017.10.030.